

On the Function and Structure of Synthetically Modified Porins**

Simon Reitz, Menekse Cebi, Philipp Reiß, Gregor Studnik, Uwe Linne, Ulrich Koert,* and Lars-Oliver Essen*

The attachment of synthetic modulators to biological ion channels is promising for applications in neurobiology and sensing.^[1] While progress has been made on the modification of channels with a narrow ion conductance pathway,^[2] the use of wider pores for ion-channel engineering has been mainly limited to hemolysin.^[1a,3] The porins offer a broad variety of β -barrel architectures with pores of variable diameters, which makes them promising candidates for attaching synthetic modulators.^[4] Unlike the oligomeric hemolysins, porins have a conductance pathway formed by a single polypeptide chain, which eases synthetic modifications in the pore interior. Herein we present functional and structural data for the implementation of synthetic modulators into the trimeric porin OmpF.

The OmpF porin from *Escherichia coli* is 340 amino acids long and has a 16-stranded antiparallel β -barrel structure (Figure 1a).^[5] Three OmpF molecules assemble to a trimer within the membrane (Figure 1b). A loop region called L3 folds inside the pore and contributes to a constriction zone. The pore of OmpF is maximally restricted at this eyelet to an elliptical cross section of 7×11 Å and allows passage of

molecules up to 600 Da with minor ion specificity. The N-terminal region covering β strands 1 and 16 was selected for synthetic modifications. Within this region the sidechain of Lys16 faces the constriction zone and was therefore chosen as a suitable attachment point for synthetic modulators (Figure 1a).

Two different synthetic routes were examined for the covalent attachment of a modulator within the OmpF channel (Scheme 1): protein semisynthesis combined with azide/alkyne click chemistry (Route A) and introduction of a cysteine residue by mutation with subsequent *S*-alkylation (Route B).

Route A (protein semisynthesis by native chemical ligation, NCL) required the preparation of an N-terminal fragment thiol ester and a C-terminal fragment bearing an N-terminal cysteine residue, which is crucial for NCL. The N-terminal fragment **1**, in which Lys16 was altered to propargyltyrosine ether Π (K16II), was synthesized by fluorenylmethoxycarbonyl (Fmoc) solid-phase synthesis. A Cu^I-catalyzed cycloaddition of the alkyne **1** with the dansyl azide **2**, which was used as a reporter group, gave the peptide **3**. The C-terminal OmpF fragment **4**, which lacks the first 26 amino acids and harbors the N27C mutation, was produced as inclusion bodies using a porin-deficient *E. coli* strain. The ligation between the thiol ester **3** and the N-terminal cysteine of **4** to the OmpF hybrid **5** proceeded under denaturing conditions with similar yields (50%) as with the native analogue of **4** harboring a lysine residue at position 16 (60%), as judged by sodium dodecylsulfate polyacrylamide gel electrophoresis (SDS-PAGE). The starting point for Route B was the OmpF mutant **6** in which Lys16 is replaced by a cysteine residue (K16C). The *S*-alkylation with the iodoacetamide-activated dansyl derivative **7** provided the OmpF hybrid **8** in nearly quantitative yields (above 90%).

The resulting OmpF hybrids **5** and **8** were refolded by insertion into mixed unilamellar vesicles comprising a 1:1 ratio of 1,2-dimyristoyl-*sn*-glycero-3-phosphocholine and *n*-dodecyl- β -D-maltoside using the procedures established for the unmodified OmpF protein.^[5] Despite the presence of the bulky dansyl groups within the pore, the refolding yields were similar to unmodified OmpF (up to 70%), as judged by the emergence of SDS-resistant OmpF trimers in SDS-PAGE gels.^[6] Like unmodified OmpF, the hybrids **5** and **8** could be further purified from unfolded protein by trypsin digestion exploiting the overwhelming stability of intact OmpF trimers against proteolytic digestion.

The functional consequences of porin modifications were studied by conductance measurements at high salt concentrations in order to focus solely on blockage efficiencies rather than on effects caused by slight differences of channel

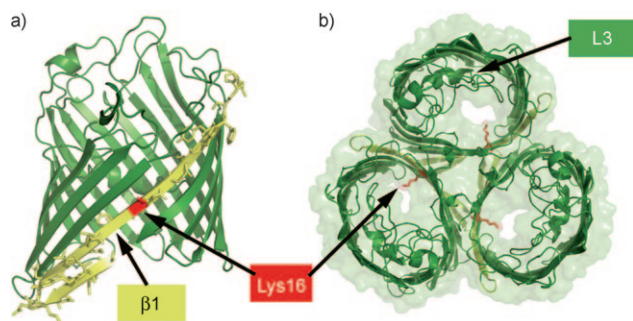
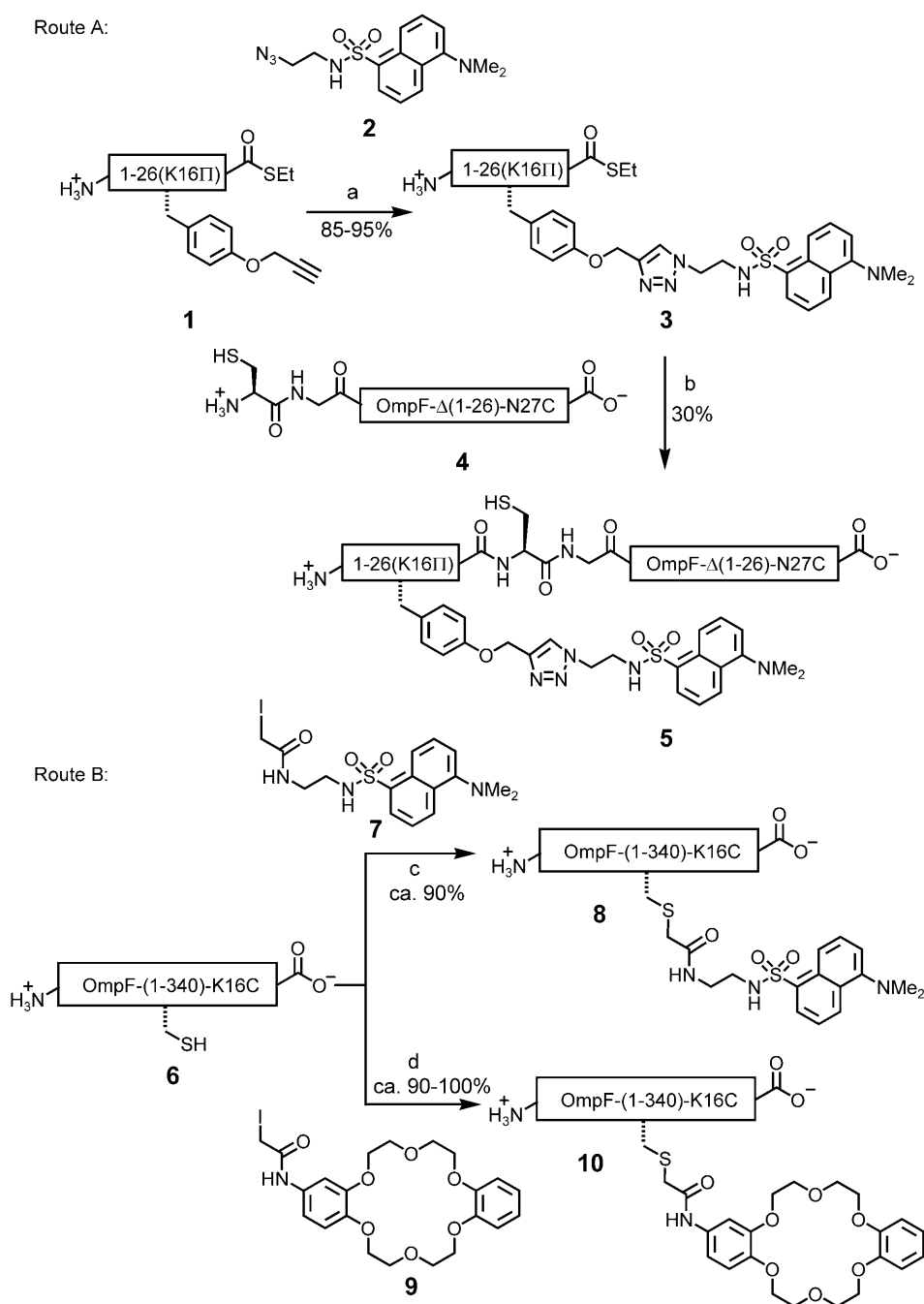


Figure 1. Structure of OmpF. a) Side view of the OmpF monomer. The peptide stretch used for native chemical ligation ($\beta 1$) is marked in yellow; the attachment site for synthetic modulators (Lys16) is shown in red. b) Top view of the OmpF trimer with the loop region L3.

[*] S. Reitz, M. Cebi, P. Reiß, G. Studnik, U. Linne, Prof. Dr. U. Koert, Prof. Dr. L.-O. Essen
Fachbereich Chemie, Philipps-Universität Marburg
Hans-Meerwein-Strasse, 35032 Marburg (Germany)
Fax: (+49) 6421-282-5677
E-mail: koert@chemie.uni-marburg.de
essen@chemie.uni-marburg.de

[**] Support from the DFG and the Volkswagen Foundation is gratefully acknowledged.

Supporting information for this article is available on the WWW under <http://dx.doi.org/10.1002/anie.200900457>.



Scheme 1. Synthesis of OmpF derivatives with covalently attached modulators at position 16. Route A: a) Cu^I-catalyzed [3+2] click chemistry; b) native chemical ligation under denaturing conditions in 8 M urea. Route B: S-alkylation of OmpF-K16C with c) dansyl iodoacetamide **7** and d) dibenzo-[18]crown-6 derivative **9**, performed under denaturing conditions in 6 M urea. For further experimental details, see the Supporting Information.

electrostatics.^[7] Using the black lipid membrane (BLM) technique, porin-trimer measurements were first performed at +140 mV, where individual closure of single pores within the OmpF trimer can readily be tracked (Figure 2).^[8] Moreover, current-voltage (*I/U*) curves were recorded and analyzed (−160 to 160 mV). For the dansyl triazole derivative **5**, no significant change in the trimer conductance was observed (**5**: (51.5 ± 6.0) pA; OmpF: (51.2 ± 3.0) pA; Figure 2 a). The *I/U*

U curves for recombinant full-length OmpF, wild-type OmpF generated by NCL, and OmpF hybrid **5** showed no significant differences. This result indicated that 1) NCL is indeed a valid route to assemble native-like OmpF polypeptides and 2) introduction of a conductance modulator of a molecular mass of 319 Da near the constriction zone of OmpF is not sufficient to alter its conductance.

In contrast, the cysteine-linked dansyl-OmpF hybrid **8** showed an unusual, large spread for its trimer conductances (see the Supporting Information), which was observed neither for refolded wild-type OmpF (Figure 2d) nor for its mutants or OmpF hybrid **5**. This finding may indicate conformational mobility and/or heterogeneity of the synthetic modulator within the pore of **8**. *I/U* curve analysis revealed that the average specific conductance of hybrid **8** is diminished by 15 % ((0.78 ± 0.02) nS) compared to unmodified **6** ((0.92 ± 0.02) nS). Inspection of trimer events likewise demonstrated the reduction of conductivity for **8** (Figure 2b). The lack of significant change, as found for **8**, for hybrid **5** points to the crucial role of the nature of the chemical linkage for the function of hybrid ion channels. The size difference between the modulating groups in **5** and **8** (451 vs. 377 Da) is not large enough to rationalize this result alone. Obviously, the synthetic modulator of **5** cannot occupy the central constriction zone of OmpF, instead adhering most likely to the inner wall of the OmpF pore, whereas in **8** the constriction site is at least partly blocked.

To address this theory in more detail, another OmpF hybrid **10** was synthesized, for which Route B was used to attach the dibenzo-[18]crown-6 derivative **9** to the OmpF-K16C mutant **6**. *I/U* curve analysis revealed that the OmpF hybrid **10** shows very similar properties to **8**, including a specific conductance reduction by 18 % ((0.75 ± 0.01) nS) and a large spreading of individual trimer conductances in its *I/U*

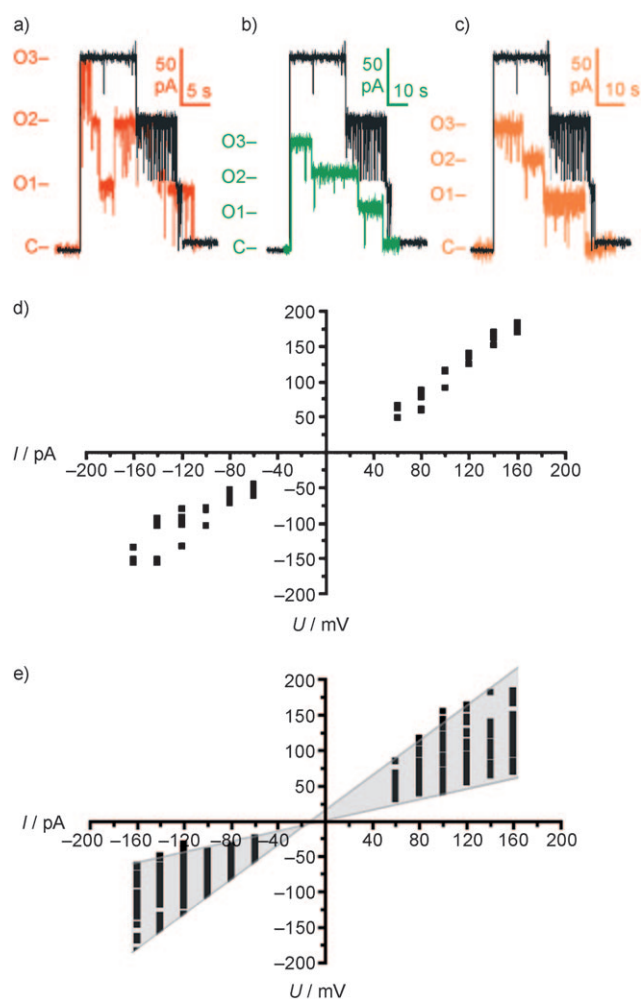
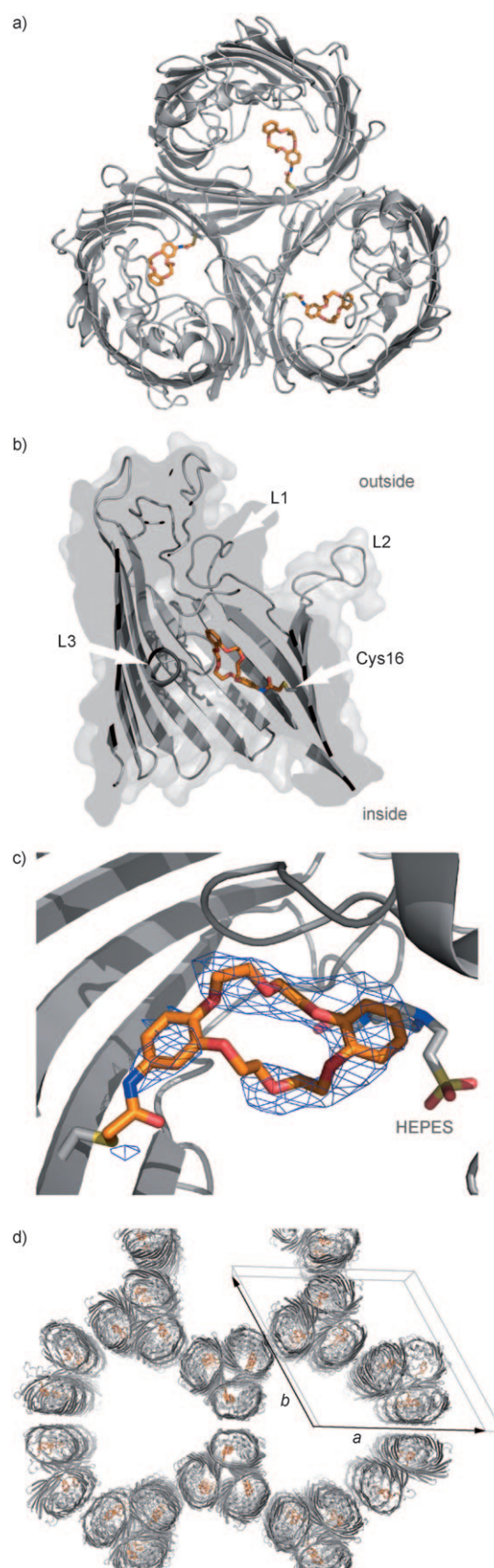


Figure 2. Ion-channel conductances by OmpF hybrids. a)–c) Current trace of an OmpF trimer (black) and a) the dansyl hybrid **5** (red), b) the dansyl hybrid **8** (green), and c) the crown ether modified hybrid **10** (orange). BLM measurements were performed in 150 mM KCl at 140 mV. Numbers on the left refer to the number of open monomers (C = closed, O = open). d), e) Current–voltage measurements for d) OmpF and e) hybrid **10**.

curves (Figure 2e) with limiting conductances of 0.42 and 1.14 nS. Inspection of single trimer events likewise demonstrated the reduced conductivity for **10** (Figure 2c).

For **10**, the structural consequences of its modification could be studied by X-ray crystallography, as two trigonal crystal forms were obtained, each comprising one molecule per asymmetric symmetry unit. Crystal form I diffracted to 3.2 Å resolution and corresponded to the known crystal form of OmpF^[5c] but lacked ordered density for the synthetic modulator.

Figure 3. Crystal structure of the OmpF hybrid **10**. a) Top view of the OmpF trimer **10** highlighting the dibenzo-[18]crown-6 moiety (orange). b) Side view of the cross-section of **10**. c) SIGMA-weighted $F_{\text{obs}} - F_{\text{calc}}$ difference density map calculated at 3.4 Å resolution for the dibenzo-[18]crown-6 moiety (contouring level 2.7 σ). Note the 2-(4-(2-hydroxyethyl)-1-piazinyl)-ethanesulfonate (HEPES) molecule below the syn-



thetic modulator. d) Crystal packing of the novel OmpF crystal form indicating the quasi-continuous arrangement of OmpF trimers along the *c* axis.

Crystals of form II were obtained from the same protein batch as form I and diffracted to 3.4 Å resolution. This crystal form has not been observed to date for OmpF^[5c,9] but it could be solved by molecular replacement (PDB code 3FYX). This is first structure of a pore partly blocked by a synthetic modulator. As in crystal form I, the OmpF trimers associate to columnar structures along the *c* axis by interaction of their loop structures (Figure 3d).

The protein conformations within the two crystal forms are the same, but in crystal form II there is significant difference electron density in the ion conductance pathway of the OmpF channel. One density feature corresponds to the dibenzo-[18]crown-6 moiety emanating from C16 and transverse the constriction zone of OmpF (Figure 3a–c). Another portion of the difference electron density could be assigned to a HEPES buffer molecule whose sulfonate group electrostatically interacts with the basic patch of the OmpF pore interior (Lys80, Arg132, Arg167, Arg168). The conformation of the rather flexible dibenzo-[18]crown-6 moiety is generally butterfly-like,^[10] but it appears to be severely distorted in the constriction zone in **10** (Figure 3c). Its polyoxyethylene ring spans the constriction zone such that one part of the ring with its ethylene oxygen atoms is close to the basic sidechains of Arg42, Arg82, and Arg132 along the inner porin channel wall, while the other part is close to the acidic sidechains of Asp113 and Glu117 derived from the L3 loop (Figure 4a). The distal aryl group of the crown ether forms several van der Waals interactions with the surface of the L3 loop involving the sidechains of Tyr102, Tyr106,

Asp113, Ala123, and Arg132 and thereby closely approaches the HEPES molecule bound next to it.

Overall, the crystal structure of the OmpF hybrid **10** shows that a wide-pore channel such as OmpF that has been modified by a synthetic modulator can occupy a uniformly closed state, although individual trimers of the hybrid exhibit divergent conductance properties. Given the lack of ordered density for the crown ether moiety in crystal form I, we may conclude that the form II structure of **10** represents a conformational snapshot that was serendipitously stabilized by the chosen crystallization conditions.

A view of the cross-section of **10** (Figure 4b) shows that the blocked conformation requires a stretched, inward-oriented conformation of the crown ether so that it is partly contacting the L3 loop (blocked conformation). An alternative conformation in which the crown ether is pointing away from the constriction zone would provide significantly more conformational freedom to the synthetic modulator (loosened conformation) but would abolish pore blockage.

If interconversion between blocked and loosened conformations of the synthetic modulator is hindered by steric interference, for example with loop L3, the observed heterogeneous channel conductances would arise solely from conformational heterogeneity. The nature of the linker between the crown ether and position 16 on β strand 1 might then be of utter importance; for example, OmpF hybrid **5** could adopt only an outward conformation for its synthetic modulator owing to the longer and stiffer tyrosyl-triazole linker and would hence be arrested in the open state. Conformational heterogeneity of hybrid ion channels was previously thought to arise mainly from intrinsic properties of the protein template employed.^[11] As we show that the interplay of synthetic modulator and protein template is crucial for conformational heterogeneity, we may conclude that single-site attachment of a synthetic modulator is not necessarily sufficient in wide-channel porins but that additional noncovalent interactions or second-site attachments are necessary to implement effective pore blockage. The results obtained herein from the synthetic modulation of OmpF should be of general use for future ion-channel engineering efforts in the β -barrel porin area.

Received: January 23, 2009

Published online: March 25, 2009

Keywords: crown compounds · ion channels · native chemical ligation · porin structures · ion-current modulators

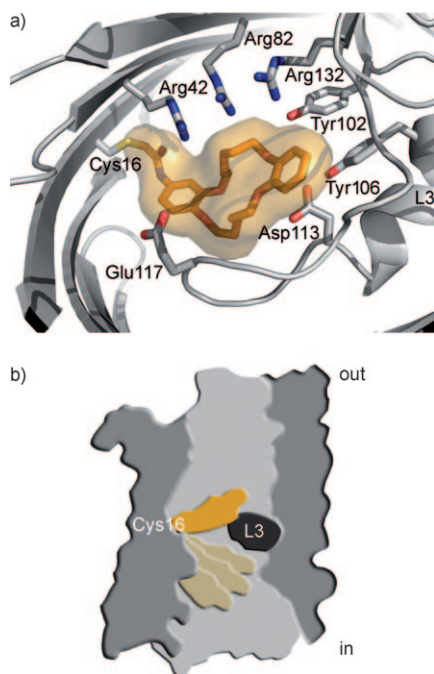


Figure 4. Blockage of the constriction zone within the OmpF hybrid **10**. a) Surface representation for the dibenzo-[18]crown-6 compound between the L3 loop and the basic amino acids. b) Schematic representation of blocked (orange) and loosened (light yellow) conformations for the synthetic modulator of **10** in the OmpF pore.

- [1] a) H. Bayley, L. Jayasinghe, *Mol. Membr. Biol.* **2004**, *21*, 209–220; b) M. R. Banghart, M. Volgraf, D. Trauner, *Biochemistry* **2006**, *45*, 15129–15141; L.-O. Essen, U. Koert, *Ann. Rep. RSC* **2008**, *104*, 165–188.
- [2] a) F. Valiyaveetil, M. Sekedat, T. W. Muir, R. MacKinnon, *Angew. Chem.* **2004**, *116*, 2558–2561; *Angew. Chem. Int. Ed.* **2004**, *43*, 2504–2507; b) F. Valiyaveetil, M. Sekedat, T. W. Muir, R. MacKinnon, *J. Am. Chem. Soc.* **2006**, *128*, 11591–11599; c) A. Koçer, M. Walko, W. Meijberg, B. L. Feringa, *Science* **2005**, *309*, 755–758; d) A. Koçer, M. Walko, E. Bulten, E. Halza, B. L.

- Feringa, *Angew. Chem.* **2006**, *118*, 3198–3202; *Angew. Chem. Int. Ed.* **2006**, *45*, 3126–3130; e) M. Banghart, K. Borges, E. Isacoff, D. Trauner, R. H. Kramer, *Nat. Neurosci.* **2004**, *7*, 1381–1386.
- [3] a) L. Q. Gu., O. Braha, S. Conlan, H. Bayley, *Nature* **1999**, *398*, 686–690; b) H. C. Wu, Y. Astier, G. Maglia, E. Mikhailova, H. Bayley, *J. Am. Chem. Soc.* **2007**, *129*, 16142–16148.
- [4] *Bacterial and Eucaryotic Porins* (Ed.: R. Benz), Wiley-VCH, Weinheim, **2004**.
- [5] a) R. M. Garavito, J. P. Rosenbusch, *J. Cell Biol.* **1980**, *86*, 327–329; b) A. Engel, A. Massalski, H. Schindler, D. L. Dorset, J. P. Rosenbusch, *Nature* **1985**, *317*, 643–645; c) S. W. Cowan, T. Schirmer, G. Rummel, M. Steiert, R. Gosh, R. A. Pauptit, J. N. Jansonius, J. P. Rosenbusch, *Nature* **1992**, *358*, 727–733.
- [6] a) T. Surrey, F. Jähnig, *Proc. Natl. Acad. Sci. USA* **1992**, *89*, 7457–7461; b) T. Surrey, A. Schmid, F. Jähnig, *Biochemistry* **1996**, *35*, 2283–2288.
- [7] A. Alcaraz, E. M. Nestorovich, M. Aguilera-Arzo, V. M. Aguilera, S. M. Bezrukov, *Biophys. J.* **2004**, *87*, 943–957.
- [8] A. Engel, A. Massalski, H. Schindler, D. L. Dorset, J. P. Rosenbusch, *Nature* **1985**, *317*, 643–645.
- [9] E. Yamashita, M. V. Zhalnina, S. D. Zakharov, O. Sharma, W. A. Cramer, *EMBO J.* **2008**, *27*, 2171–2180.
- [10] a) R. Hilgenfeld, W. Saenger, *Angew. Chem.* **1981**, *93*, 1082–1085; *Angew. Chem. Int. Ed. Engl.* **1981**, *20*, 1045–1046; b) A. N. Chekhlov, *Russ. J. Coord. Chem.* **2000**, *27*, 771–775; c) J. W. Steed, *Coord. Chem. Rev.* **2001**, *215*, 171–221.
- [11] M. Chen, S. Khalid, M. S. P. Sansom, H. Bayley, *Proc. Natl. Acad. Sci. USA* **2008**, *105*, 6272–6277.